

Biofouling and corrosion rate of welded Nickel Aluminium Bronze in natural and simulated seawater

Tamsin Dobson, Anna Yunnie, Dimitrios Kaloudis, Nicolas Larrosa & Harry Coules

To cite this article: Tamsin Dobson, Anna Yunnie, Dimitrios Kaloudis, Nicolas Larrosa & Harry Coules (2024) Biofouling and corrosion rate of welded Nickel Aluminium Bronze in natural and simulated seawater, *Biofouling*, 40:2, 193-208, DOI: [10.1080/08927014.2024.2326067](https://doi.org/10.1080/08927014.2024.2326067)

To link to this article: <https://doi.org/10.1080/08927014.2024.2326067>



© 2024 The Author(s). Published by Informa UK Limited, trading as Taylor & Francis Group



[View supplementary material](#)



Published online: 08 Mar 2024.



[Submit your article to this journal](#)



Article views: 1228



[View related articles](#)



[View Crossmark data](#)



Citing articles: 3 [View citing articles](#)

Biofouling and corrosion rate of welded Nickel Aluminium Bronze in natural and simulated seawater

Tamsin Dobson^a, Anna Yunnice^b, Dimitrios Kaloudis^b, Nicolas Larrosa^a and Harry Coules^a

^aSolid Mechanics Research Group, University of Bristol, Bristol, UK; ^bPML Applications Ltd., Plymouth Marine Laboratory, Plymouth, UK

ABSTRACT

Updated understanding on the effect of biofouling on corrosion rate is needed to protect marine structures as climate change is altering seawater physiochemistry and biofouling organism distribution. Multi-disciplinary techniques can improve understanding of biofouling development and associated corrosion rates on metals immersed in natural seawater (NSW). In this study, the development of biofouling and corrosion on welded Nickel Aluminium Bronze (NAB) was investigated through long-term immersion tests in NSW, simulated seawater (SSW) and air. Biofouling was affected by geographic location within the marina and influenced corrosion extent. The corrosion rate of NAB was accelerated in the initial months of exposure in NSW (1.27 mm.yr^{-1}) and then settled to 0.11 mm.yr^{-1} (annual average). This was significantly higher than the 0.06 mm.yr^{-1} corrosion rate measured in SSW, which matched published rates. The results suggest that corrosion rates for cast NAB should be revised to take account of biofouling and updated seawater physiochemistry.

ARTICLE HISTORY

Received 10 November 2023
Accepted 24 February 2024
Published Online 8 March 2024

KEYWORDS

Biofouling; corrosion rate; testing environments; immersion tests

Introduction


Biofouling is ubiquitous in the marine environment and is a large concern for the marine industry as it can increase costs and reduce the operational lifespans of immersed structures (Vinagre et al. 2020). Impacts of biofouling on marine operations include the loss of performance due to increased drag (Schultz 2007) and the obstruction of sea valves, heat exchangers or sensors (Delauney et al. 2010). Flemming (2011) estimated the annual cost to the combined marine industries due to microbial biofouling to be over US \$15 billion.

Marine biofouling is a multistage process that is usually initiated by the development of a biofilm on the immersed surface (Zobell and Allen 1935; Railkin 2004). Biofilms are known to substantially change the local chemistry of the surface that they attach to including affecting local pH, oxygen concentrations, organic and inorganic species (Little and Lee 2007). After one month immersed in natural seawater (NSW), the chemicals released by biofilm organisms encourage larvae and spores to attach and grow (Railkin 2004). Within a few weeks or months,

macrofouling organisms (such as sea squirts (Ascidians), Hydroids, sponges and barnacles) will also attach (Vinagre et al. 2020). Due to this, materials intended for immersion in NSW must be carefully selected for their physical properties and for their corrosion behaviour, when exposed to the complex interacting effects of biofouling (Dexter 1993).

Nickel Aluminium Bronze (NAB) is used extensively in the marine industry for components immersed in seawater. This is due to its high strength and good corrosion resistance in seawater when compared to metals such as carbon steels, brasses and pure copper (Ahmad 2006). Copper is the largest chemical component of NAB with a compositional percentage of 76.5–85.5% (Richardson 2016). From a biological perspective, copper is an essential metal that only becomes toxic to plants and micro-organisms at high concentrations (Yruela 2005). This toxicity is used in antifouling coatings (e.g. Cerchier et al. (2020)) and copper can prevent the metamorphosis of juvenile barnacles by preventing calcification of their outer shell (Pyefinch and Mott 1948). However, when immersed in NSW, copper alloys still

CONTACT Tamsin Dobson  Tamsin.dobson@bristol.ac.uk

 Supplemental data for this article can be accessed online at <https://doi.org/10.1080/08927014.2024.2326067>.

This article has been republished with minor changes. These changes do not impact the academic content of the article.

© 2024 The Author(s). Published by Informa UK Limited, trading as Taylor & Francis Group

This is an Open Access article distributed under the terms of the Creative Commons Attribution License (<http://creativecommons.org/licenses/by/4.0/>), which permits unrestricted use, distribution, and reproduction in any medium, provided the original work is properly cited. The terms on which this article has been published allow the posting of the Accepted Manuscript in a repository by the author(s) or with their consent.

experience biofouling and microbially-induced pitting corrosion (Booth 1964; Little et al. 1988; 1989; Kushkevych et al. 2021).

Interactions between biofouling and corrosion need to be understood to enable the development of new antifouling and antifouling coating schemes that prevent corrosion and biofouling simultaneously. Thus, quantifying corrosion rates and biofouling cover for uncoated copper alloys is of interest both for surveying components as part of normal maintenance activities and evaluating antifouling and corrosion protection technologies.

When NAB is immersed in corrosive media (such as seawater), localised corrosion occurs when the passivation layer breaks down, allowing accelerated corrosion at discrete sites (Frankel 1998). NAB is vulnerable to Selective Phase Corrosion (SPC) when immersed in natural seawater (Neodo et al. 2013; Richardson 2016) especially underneath biofouling and corrosion product deposits. SPC in NAB is classically reported as the accelerated dissolution of the copper-rich α phase within the α - κ_{III} eutectoid, due to the more negative electrode potential of the α phase compared to the κ_{III} phase (Culpan and Foley 1982). Oakley et al. (2007) observed a higher general and local corrosion rate in once-through flowing natural seawater immersed samples compared to samples in recirculating tanks of Portland Harbour seawater. To support this, a recent review of corrosion and biofouling by Vuong et al. (2023) highlighted the need to use holistic, multi-disciplinary approaches to understand biofouling drivers of corrosion.

Previous corrosion studies of NAB in seawater carried out by Culpan and Foley (1982) and Schüssler and Exner (1993) improved our understanding of the corrosion performance of this alloy in the absence of biofouling. Some studies have included the effect of galvanic coupling on NAB corrosion, showing that pitting corrosion can occur in NAB coupled to Stainless Steel (Krogstad and Johnsen 2017) and other metals (Wharton et al. 2005), highlighting the increased complexity of these interactions when a biofilm is also present. Other studies have considered biofilm or microfouling effects in isolation (Characklis 1989; Beech and Sunner 2004; Little et al. 2008; Procópio 2019), improving understanding of the bacteria-metal interface. However, these do not consider the interacting variables such as macrofouling, tide and wind forces, seawater chemical composition, temperature and salinity. Studies that consider the effect of biofilms on the corrosion process often used simulated seawater (SSW) with added nutrients

and microorganisms (Dexter 1988; Webster and Newman 1994). However, these tests proved unreliable as added media often contain anions (which can inhibit local corrosion) and yeast extract (which can interfere with electrochemical measurements), plus, the deaeration of SSW under testing conditions can produce environments that inhibit SRB growth (Little et al. 2008). For these reasons, corrosion rates measured in the laboratory often differ from those measured in natural seawater in the marine environment (Videla et al. 2005). Large variations in corrosion severity are reported in long-term NSW immersion tests (Wharton et al. 2005; Oakley et al. 2007; Krogstad and Johnsen 2017). These studies focus on corrosion severity and do not specifically consider the effect of the biofilm or biofouling organisms or include welded samples.

Welds are often the most vulnerable part of a structure, not just for corrosion, but also for load induced fracture. The corrosion of weldments can include galvanic corrosion between parent and weld material, pitting corrosion in the HAZ and residual stress effected areas, crevice corrosion due to weldment geometry and stress corrosion cracking (Aljohani et al. 2023). In NAB, heating and cooling during welding enables the development of the β -phase in the HAZ and this phase is prone to selective phase corrosion (Cobo et al. 2022).

The physiochemistry of NSW is changing due to climate change: effects such as reduced pH (Feely et al. 2009) and increased temperature (Maul et al. 2001) have been observed and the availability of fouling organisms is changing with it (Meng et al. 2019). As highlighted in a review by Vuong et al. (2023), it is important that new, multi-disciplinary, NSW corrosion and biofouling tests are carried out to take these interacting physiochemical changes into account so that marine structures and components can be protected. This paper presents a multidisciplinary long-term immersion study of plasma welded NAB in NSW, SSW, and air, investigating the development of biofouling and corrosion.

Materials and methods

NAB coupons were bead-on-plate plasma welded and immersed in one of three environments: natural seawater (NSW in Millbay Marina, U.K.), simulated seawater (SSW) or air. The physical parameters of each environment were periodically monitored. Each month the coupons were photographed and weighed. The photographs were used to map the development of corrosion and biofouling. A thematic coding

method was developed to quantify the photographic output as the percentage surface area cover of each theme. This was analysed to consider the relationship between corrosion and biofouling. The NSW coupons were assessed for biofilm density and the presence of SRB to consider the effect of bacterial cover on corrosion rate. Corrosion rates were evaluated and compared between immersion environments.

Nickel Aluminium Bronze and welding

Coupons of cast NAB were manufactured in accordance with Def Stan 02-747 Part 2 (Ministry of Defence 2013) meeting the requirements for Defence Standard 02-833 Part 2 Issue 4 (Ministry of Defence 2018) (Al-9.14, Fe-4.38, Ni-4.84, Mn-0.09, Cu-balance wt%, $\sigma_{0.2} = 265$ MPa). The coupons were sized with thickness = 30 mm and diameter = 200 mm to present a large enough surface that enabled typical marine biofouling organisms to attach (First et al. 2014). The coupons were polished to $R_a = 3.2$ to represent the standard commercial machine finish (Xometry 2018) and to remove the potential for crevice

Table 1. Plasma welding parameters.

Description	Parameter
Pure Argon gas flow rate	10 L.min ⁻¹
Plasma gas flow rate	0.8 L.min ⁻¹
Stand up distance	8 mm
Nozzle diameter	3.9 mm
Wire diameter	0.8 mm
Trailing shielding Ar gas	40 L.min ⁻¹
Current	180 A
Travel Speed	4 mm.s ⁻¹
Wire feed speed	5 m.min ⁻¹

corrosion in the ridges of the saw cuts (Dobson et al. 2022).

Before welding, each NAB coupon was preheated to 250 °C. The plasma welding process was front wire feeding, plasma torch shielding and trailing shielding. The welding wire used was 1.2 mm diameter SIFMIG 44 from SIG Consumables (Cu6328 EN 14640). Each sample was plasma welded in a bead-on-plate geometry using the parameters described in Table 1.

Natural sea water (NSW) immersion environment

Twelve (12) NAB coupons were immersed in natural seawater (NSW) at Millbay Marina (Plymouth, UK), Figure 1, from December 2021. The coupons were suspended at 1 m depth with the welded surface facing downwards to replicate the underside of a marine vessel. Six coupons remained immersed for 18 months whilst six were removed after 12 months.

Physical environmental data (including salinity, temperature, pH, dissolved oxygen and chlorophyll concentration) were measured weekly, at 1-2 m depth at the centre of the middle site (Figure 1), using a Aquameter Aquaprobe AP-5000. Millbay Marina pilings were sandblasted after 6 months of immersion for a period of 3 months (June - August 2022). This produced a black deposit of polyamine adduct cured epoxy (Sigmashield 880, conforming to BS EN ISO 12944-6: 2018) that settled on many of the coupons. The sandblasting vibrations were kept within UK HSE recommended limits. As such, the noise and vibrations were not considered to effect the study although they may have had a short term effect on local marine organisms during operations (Chahouri et al. 2022).

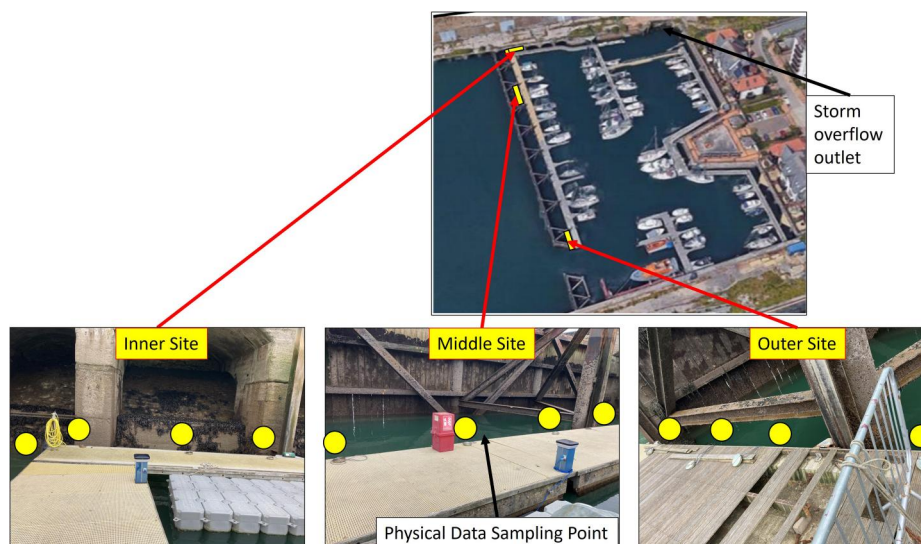


Figure 1. Deployment locations of the twelve (12) NAB samples in Millbay Marina (each coupon location indicated by a yellow circle).

Simulated seawater (SSW) and air control test

Simulated sea water (SSW) tank was used to observe the corrosion of plasma welded NAB coupons in the absence of marine biofouling organisms. SSW was produced in accordance with ASTM D1141-98 (ASTM International 1998). The temperature was maintained close to the maximum seawater temperature (Persian Gulf, 31.3 °C predicted for 2030, (Noori et al. 2019)) as per ASTM G31-21 (ASTM 2012). The SSW salinity was maintained close to the mean for open ocean natural seawater, 35 psu in line with ASTM D1141-98 (ASTM International 1998) which was also the maximum salinity seen in Millbay Marina. Salinity was measured weekly using a portable refractometer. An automatic monitoring system (Seneye ReefTM) was used to monitor water temperature, pH and dissolved oxygen, supported by manual measurements of temperature and dissolved oxygen. The growth of green and brown algae was prevented using an algae inhibitor (Dr Tim's AquaticsTM "Re-Fresh" for reef water). Two coupons remained immersed for 18 months whilst two were removed after 12 months.

The air control test consisted of three coupons that were exposed to ambient laboratory air for a 12- or 18-month period. The air in the laboratory was maintained by university wide air conditioning and measured monthly. Two coupons remained exposed for 18-months whilst one was removed after 12-months.

Corrosion and biofouling mapping

The coupons were removed from the immersion environment (NSW, SSW or air) on a monthly basis to monitor mass and surface corrosion. Masses were measured to the nearest 10 g using a calibrated electronic scale (Hanwell 50 kg Luggage Scale) and the coupons were photographed using consistent equipment, position, and distance.

Photographs of the coupons taken at 2-month intervals were identified as sufficient to show corrosion and biofouling trends in the photographic data series. A thematic coding method was developed to allow quantification of the photographic output by measuring the percentage surface area cover of each theme. The themes used in this study were: Ascidiens, Barnacles, Bryozoans, normal NAB surface, discolored NAB surface, corrosion products, black deposit and sediment/Hydroids (Figure S1). Photographs were taken from a standard distance, using the same iPhone SE7 camera and using body shadow to alleviate reflection from sunlight (to create similar light

conditions for all images). The images were analysed with Photoshop (Adobe Inc, San Jose, CA, USA), using standardised "colour select" algorithms for each theme except for Ascidiens, Barnacles and Bryozoans, which were selected manually (due to colour variability). This method was repeated, with the weld material taken as an isolated image, to investigate the different corrosion and biofouling patterns on the base material compared to the weld material.

Biofilm density analysis and tests for Sulphate reducing bacteria (SRB)

An additional plasma welded NAB coupon was immersed at the middle site of Millbay Marina in January 2023 and removed in March 2023. This 2-month immersion period allowed biofilm development before macrofouling species settled and before significant corrosion product had time to build-up.

To measure biofilm density, 12 swabs were placed in an oven (60 °C for 2 h) and then weighed using a high-resolution scale (± 0.1 mg, Sartorius R200D, Germany). The dried and weighed swabs were then used to sample regions of interest: the weld ($n=3$), weld toe ($n=3$) or base material ($n=3$). Each swabbed area was photographed with a ruler in the image to provide a size reference, and the sampled area was estimated. The final 3 swabs were used as air control samples to take account of moisture changes on the swabs.

After sampling, all 12 swabs were immediately placed back into the oven for re-drying (60 °C for 36 h). On removal from the oven the swabs were re-weighed and the difference in mass before and after swabbing was calculated. Any difference in moisture content in the dried swabs before and after sampling was considered by subtracting the average difference in mass of the air control swabs from each sample mass change. This "moisture calibrated" mass difference was taken as the mass of the biofilm for each swab. The density of the biofilm in each case was calculated by dividing the biofilm mass by the sampled area for each swab.

To confirm the presence of SRB, 18 further swabs were used. Swabs were taken of the weld ($n=4$), weld toe ($n=4$) and base material ($n=4$), swabs were also taken of the seawater close to the coupon ($n=3$) and taken as air control samples ($n=3$). After sampling, the swabs were immediately thrust into an iron sulphite agar (Sig Tests®, ECHA Microbiology Ltd., U.K.) and left in an incubator at 35 °C for 5 days.

Blackening around the swab was a positive result for the presence of SRB (ECHA 2016).

Coupon cleaning and microscopy

After immersion, the coupons were removed from their test environment and cleaned as per ASTM G1 (ASTM 1985). This allowed the extent of corrosion underneath the corrosion products and biofouling layer to be measured. Some of the samples were imaged using scanning electron microscopy (SEM). Corrosion products were sampled from the coupons using a scalpel and analysed using Energy Dispersive X-Ray Spectroscopy (EDX). A Hitachi TM2020Plus Tabletop Microscope (SEM only) and FEI Quanta 200 FEG-SEM (SEM and EDX) were used for this purpose.

Mass loss and corrosion rate

After immersion, the coupons were cleaned as per ASTM G1 so that overall mass loss could be calculated. From the mass loss results, the corrosion rates were calculated using ASTM G31, as replicated in Equation 1, with units corrected so that $k = 1$.

Equation 1: Corrosion Rate equation from ASTM G31, where k is a constant for unit conversion ($k = 1$), t is time of exposure in years, a is the exposed surface area in mm^2 , m is the mass loss in grammes (to the nearest 10 g) and ρ is the density of NAB in g/mm^3 .

$$CR = \frac{km}{at\rho}$$

Results

Environmental physiochemical properties

The physical properties of natural seawater (NSW) at the immersion test site (Millbay Marina, Plymouth) and in the SSW tank were recorded periodically. Figure 2 shows the monthly mean temperature, pH, salinity, dissolved oxygen and chlorophyll measured at Millbay Marina during the immersion tests.

Over the 18-month study in Millbay Marina, the average pH and dissolved oxygen were 7.94 ± 0.18 (SD) and $10.16 \pm 0.81 \text{ mg.L}^{-1}$ (SD), respectively. The chlorophyll level is an indicator of phytoplankton abundance and can be used to gauge the availability of biofouling species (as many biofouling species feed on phytoplankton e.g. the sea squirt *Ciona intestinalis* (Hackl et al. 2018) and Bryozoans (Lombardi et al.

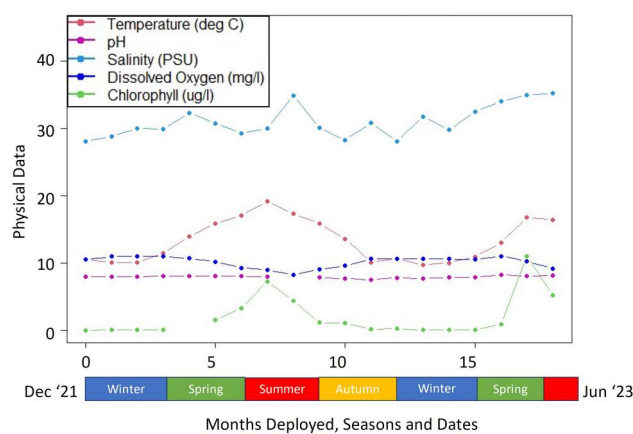


Figure 2. Monthly mean timelapse of key physical data during the 18-month immersion period at Millbay Marina (Plymouth, U.K.).

2020)). In Figure 2, a clear seasonality is seen in the chlorophyll abundance, with maximums reached during the late spring and early summer months.

The salinity, temperature, pH and oxygen levels in the SSW tank were maintained and therefore had no seasonal pattern. Over the 18-month study period, the salinity, temperature, pH and oxygen concentration varied between 34.4–36.2 psu, 27.2–32.5 °C, 8.1–8.4 pH, and 7.2–7.9 mg.L^{-1} respectively. The air temperature in the laboratory was measured to vary between 16–23 °C.

Overall biofouling and surface corrosion

Sulphate reducing bacteria (SRB) were confirmed on the base material, weld material, weld toe and in Millbay Marina seawater. SRB in the seawater suggests the presence of an SRB species with oxygen resistant proteins (Beech 2003). After 2 months immersion, the biofilm density was found to be consistent across all areas of the coupon with an average density of $20.8 \mu\text{g mm}^{-2}$ (standard error = $5.98 \mu\text{g mm}^{-2}$, $n = 12$). This is consistent with the biofilm cell density stated in a review of marine biofilms carried out by Qian et al. (2022).

The dominant biofouling organisms observed in Millbay Marina were Ascidians (predominantly *Ciona intestinalis*), Bryozoans (erect and encrusting), and Hydroids (Figure S1). Bryozoans and Hydroids are colonial organisms that are often mistaken for flora.

Photographic time-series of immersed samples in the three environments are shown in Figure 3. Using the photographic data, surface cover was analysed thematically for the 12-month immersion period, Figure 4. This shows that the surface area covered by corrosion products and biofouling organisms

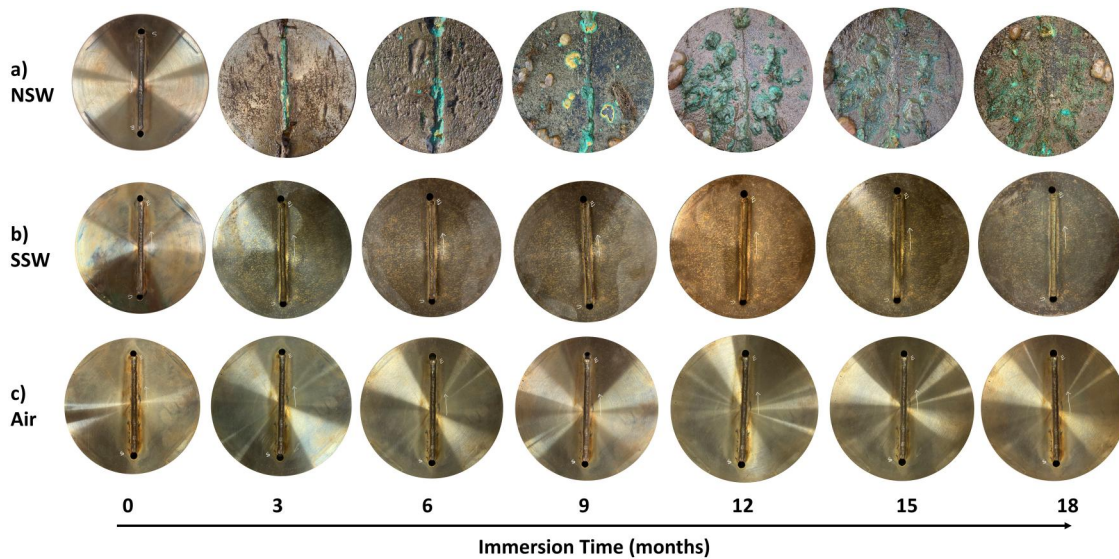


Figure 3. 3-monthly interval photographs of a) a coupon immersed in natural sea water (NSW) at the middle site of Millbay Marina (Plymouth, UK) b) a coupon immersed in simulated seawater and c) a coupon exposed to laboratory air. All coupons (as photographed) have a diameter of 200 mm.

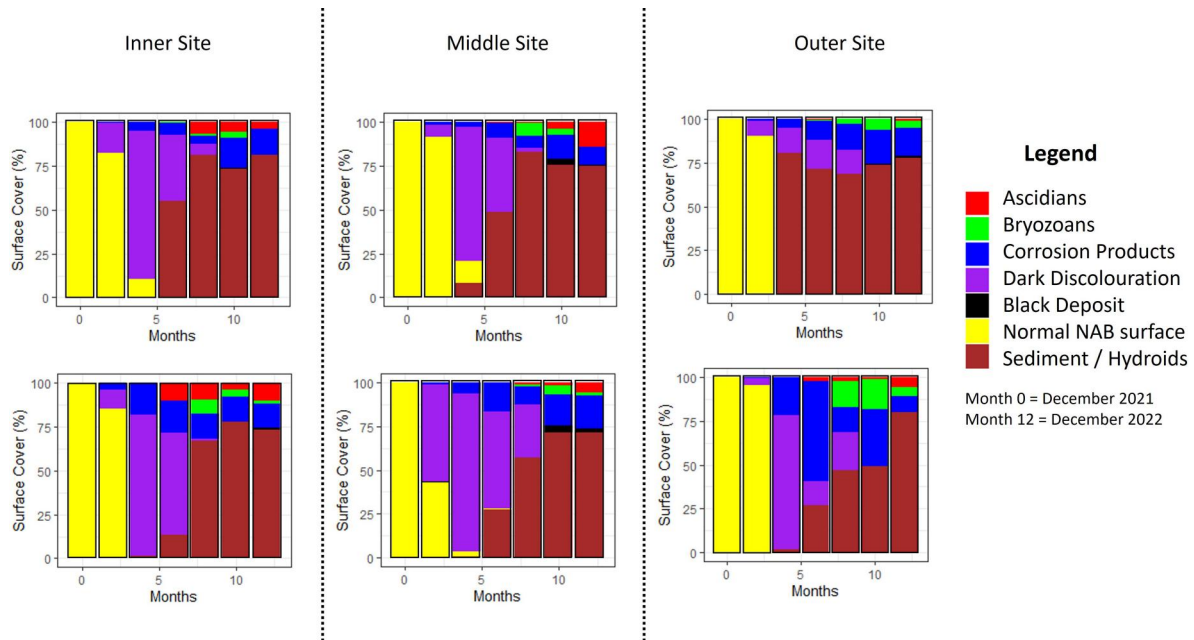


Figure 4. Surface cover measured every 2 months for the 6 coupons immersed in the inner, middle and outer sites of Millbay Marina over the initial 12-month study period. Each coupon (as photographed) has a diameter of 200 mm.

increased with time for all Millbay Marina immersion sites. After 4 months immersion, all coupons were showing at least some surface discolouration, although the surface was still dominated by “normal NAB”. Between 4-6 months of immersion the surface of all coupons darkened, patina was formed, and the first fouling organisms were observed. Between 8-12 months of immersion, the surface of most of the coupons was dominated by Hydroid growth. By the end of the 12-month immersion period, most of the coupons were covered in marine sediment and

Hydroids which completely obscured the metal surface from the photographs (Figure 3). These results show that the coupons immersed at the inner site in Millbay Marina were predominantly biofouled by solitary Ascidians whilst the coupons deployed at the outer site were predominantly biofouled by colonies of erect Bryozoans.

After 18 months immersion, the coupons were predominantly covered with sediment and Hydroids and the biofouling pattern had altered. Ascidians attached more to coupons at the outer and middle sites of

Millbay Marina (Figure 5) and calcified, adult barnacles (*Balanus crenatus*) were attached to coupons in all three sites (Figure S2). The outermost coupon (closest to the marina mouth) was observed to have the most diverse biofouling community with fast species succession, as illustrated in Figure 6.

Energy-dispersive X-ray spectroscopy (EDX) analysis was performed on two samples of the black soot deposit after 12 months immersion, Figure S3. The Na, Cl and S content represent seawater salt and sulphur content whilst the presence of Cu, Al and Fe are assumed to be caused by the introduction of corrosion products into the black soot samples. N is difficult to detect through EDX and H is not detectable (Wolfgong 2016). The high wt% of C and O is consistent with the polyamine adduct cured epoxy that was sandblasted off the pilings as this coating primarily contains epoxy resin ($C_{21}H_{25}ClO_5$) and polyamine ($N(CH_2CH_2NH_2)_3$). These results along with the timing of the black deposit appearance on the coupons, strongly suggest that the black deposit seen on the coupons is from the sandblasted piling paint.

Weld material biofouling and corrosion

Surface cover of the weld material was significantly different to the average surface cover when calculated over the coupon's entire surface, Figure 7. The weld material appeared darkened immediately after welding due to the oxide layer produced by the welding process. After 2 months immersion, the weld area showed an average of 36% cover by corrosion products compared to <1.5% average cover on the coupons overall. The maximum cover of corrosion products on the weld material is seen after 4-10 months immersion, with > 66% surface cover on the weld compared to <20% cover on the coupons overall. After 12 months

immersion, the difference in corrosion product cover on the weld material (32%) compared to the coupon as a whole (14%) remained significant. After 18 months immersion, the difference started to reduce, with corrosion products on the weld material less visible due to increased sedimentation and fouling cover.

In comparison, the weld material on coupons immersed in SSW showed significantly less corrosion cover (0% after 12 months) and corrosion product deposits on coupons immersed in SSW were only found in small, isolated deposits on the weld bead after 15 months immersion, Figure 8. No corrosion products were measurable on the air control samples.

Mass loss and corrosion rates

Figure 9 compares the mean mass loss for all immersion times and immersion environments. The 2-month mass loss data was measured from the coupon immersed in the middle site of Millbay Marina (for biofilm and SRB tests) between January - March 2022.

The changes in mass measured on coupons immersed in NSW include mass loss caused by erosion corrosion and/or tribocorrosion of material due to abrasion of the attachment rope. The volume of rope erosion was estimated from scans where the average depth, width and length of the eroded volume was measured ($n=6$). From this data, the average eroded volume (913mm^3 , $SD = 276\text{mm}^3$) was used to calculate the average mass loss through rope erosion (assuming the density of NAB to be $7.65 \times 10^{-3} \text{g}\cdot\text{mm}^{-3}$). This was calculated to be $1.4 \times 10^{-3} \text{kg}$ per coupon per year. Considering the mass change seen in Figure 10, this is considered negligible. In addition, as many NAB components that are immersed in

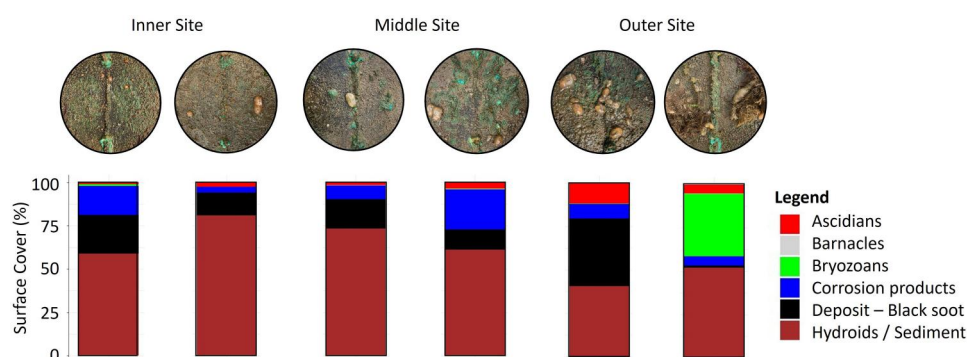


Figure 5. Surface cover on plasma welded NAB coupons after 18 months immersion in natural seawater (Millbay Marina, Plymouth, U.K.) showing the location of the coupons in the inner, middle or outer site as per Figure 2. Photographs of the coupons are shown above each month to further illustrate the biofouling cover. Each coupon (as photographed) has a diameter of 200 mm.

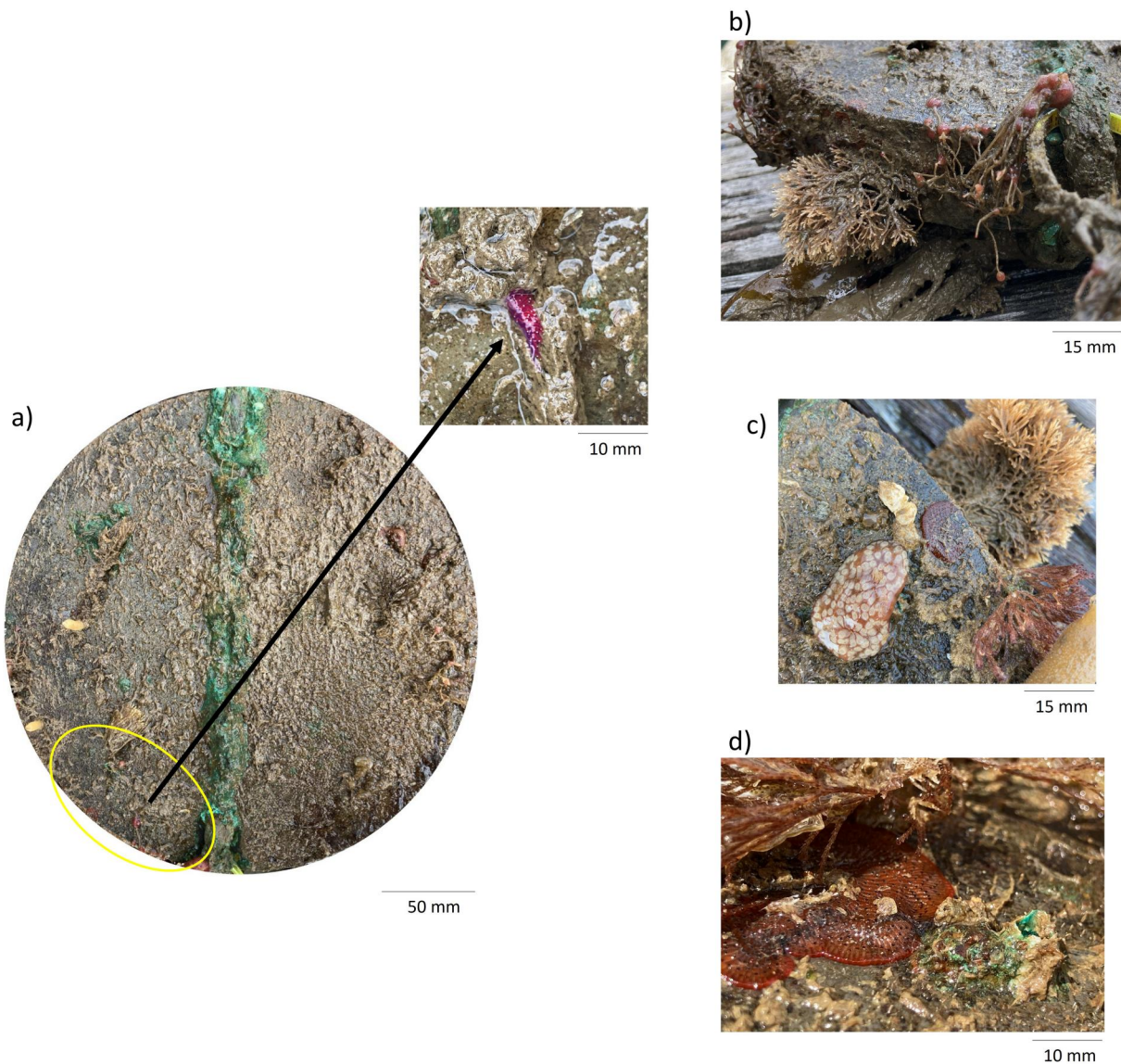


Figure 6. Species succession on the outermost coupon in months 14-18 taking one area of the coupon (highlighted in yellow) as an example. a) Whole coupon at Month 14 with a zoomed image showing a nudibranch (a mobile species). b) The yellow highlighted area at Month 16 showing the presence of a (bushy) erect Bryozoan species (*Tricellaria inopinata*) and a Hydroid species from the Tubulariidae family (stalked with red/pink heads) c) The yellow highlighted area at Month 17 showing the presence of a Star Ascidian (*Botrylloids diegensis*) and a sponge (*Sycon ciliatum*) d) The yellow highlighted area at Month 18 showing the presence of an adult barnacle (*Balanus crenatus*) with Copper oxide on its outer shell. Note that the encrusting Bryozoan (*Watersipora subatra*) seen forming in Month 14 grows during this time frame and remains *in situ* as a frame of reference.

natural seawater will experience an element of abrasion (or erosion corrosion or tribocorrosion) due to wave motion and/or mechanical wear (Wood 2017), it was considered appropriate to include this mass loss in the analysis.

Monthly mass change measurements taken during the experiment include biofouling mass (for NSW coupons) and the mass of any retained water (NSW and SSW). As such, monthly mass change measurements for the NSW immersed coupons were dominated by mass gain due to biofouling, whilst the SSW immersed coupons monthly mass change was

dominated by mass loss due to corrosion, Figure 10. The air control coupons showed no significant change in mass during the study.

The corrosion rates in air were calculated to average $<0.02 \text{ mm.yr}^{-1}$. The corrosion rates calculated from the SSW immersed coupons exactly replicate the predicted corrosion rate of 0.06 mm.yr^{-1} (The Aluminium Bronze Advisory Service 1981). However, the corrosion rates calculated for the NSW immersed coupons were, on average, 10 times higher than this and varied with immersion time. A corrosion rate of 1.27 mm.yr^{-1} was measured in the first 2 months,

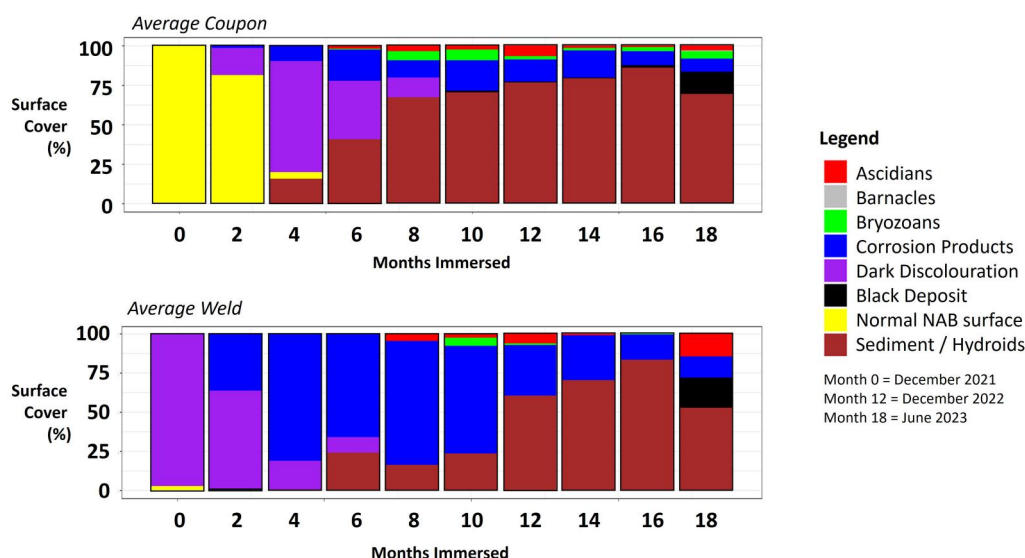


Figure 7. Surface cover for an average coupon compared to the surface cover for an average weld bead during an 18-month immersion period in natural seawater ($n = 6$).

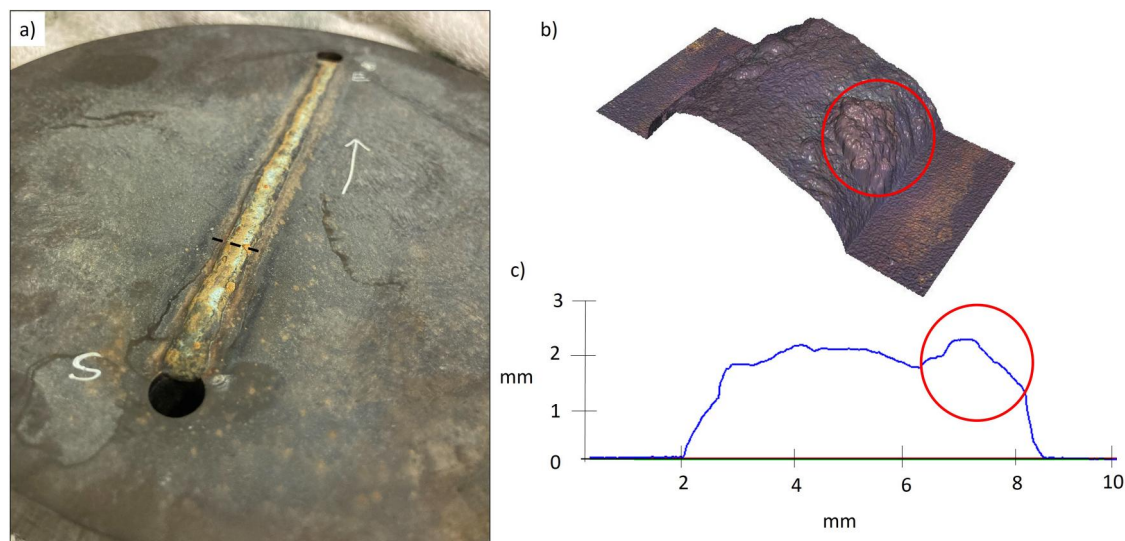


Figure 8. a) Coupon after immersion in SSW for 18 months. b) Model of the section containing the black dotted line with corrosion deposit on the weld material circled in red. c) Profile of the weld taken along the black dotted line in a) showing the corrosion product deposit heights (circled in red).

settling to a mean of 0.11 mm.yr^{-1} after 12 months, Figure S4.

Discussion

Temporal and seasonal effects on macrofouling

Millbay Marina was found to experience biofouling all year, with seasonal variation in abundance and community composition. The main biofoulers were Ascidiaceans, Bryozoans and Hydroids, however barnacles (*Balanus crenatus*) were found on the coupons after 18 months immersion. Hydroids are considered to be opportunistic species that exhibit rapid recovery

rates through both asexual reproduction and larval colonization within 6-8 weeks of settlement (Hughes 1983) and therefore their presence in this study was predicted. Ascidiaceans are a known biofouling species in Millbay and are a global fouling threat due to their rapid growth rate and ability to settle on a wide range of materials (Lambert 2007). Their proven ability to settle on copper alloys is disadvantageous.

The coupons were immersed with the welded surfacing facing down in the water to ensure that the welded face was non-illuminated. This discouraged the growth of macroalgae (which requires sunlight for photosynthesis) and the results support the research carried out by Durante (1991) and by Rius et al.

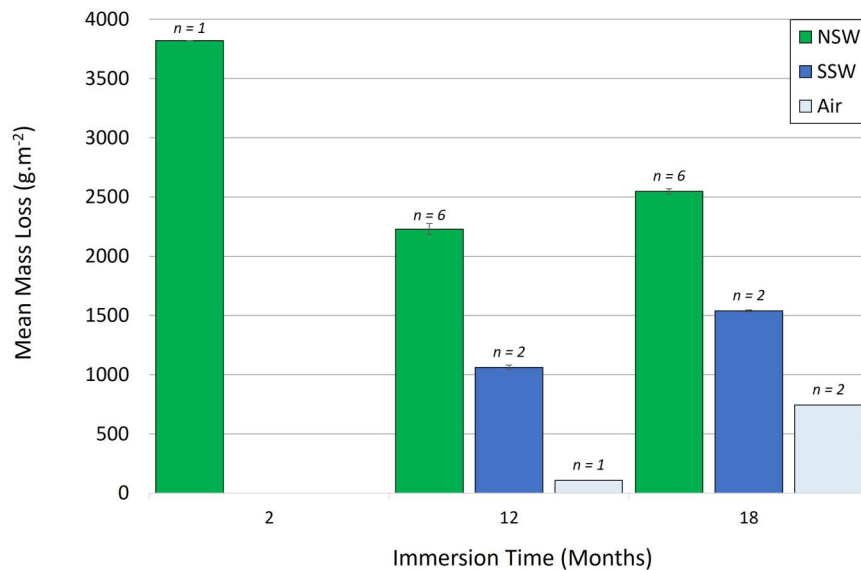


Figure 9. Mean mass loss per immersion time and immersion environment (NSW = natural seawater (Millbay Marina, Plymouth, U.K.), SSW = simulated seawater and Air = control environment, exposed to ambient laboratory air). SD shown where $n > 1$.

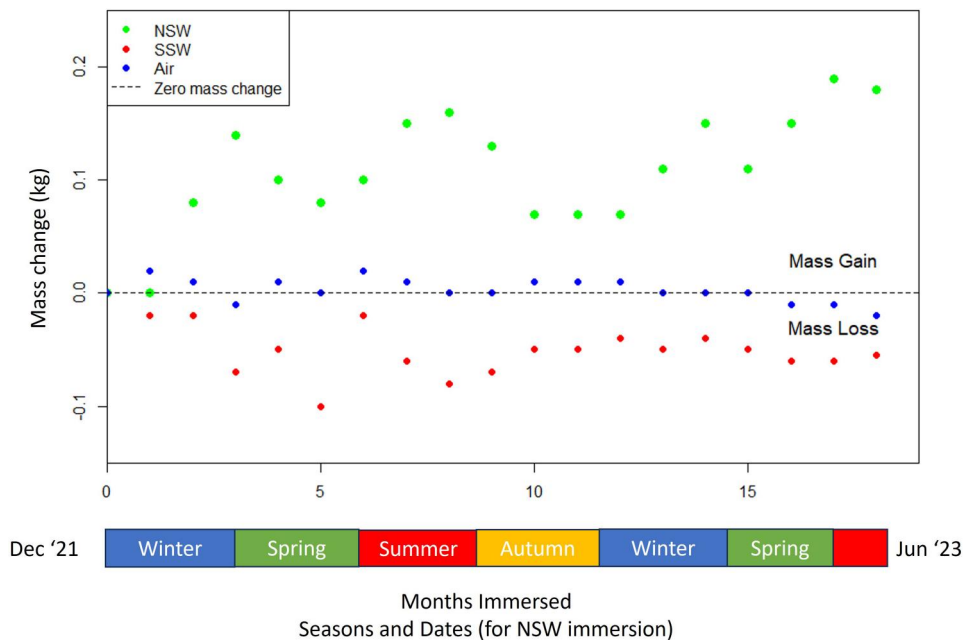


Figure 10. Mass change averaged for the coupons immersed in natural seawater (NSW), simulated seawater (SSW) and exposed to ambient air (control) per month over the 18-month study. These masses were measured during the experiment and therefore include fouling mass (for NSW coupons) and any retained water (NSW and SSW coupons).

(2010) showing that most Ascidiens will preferentially settle on non-illuminated surfaces.

Two seasonal peaks in mass gain were seen for the NSW immersed coupons in the spring (months 3-4) and summer (months 7-8), Figure 10, caused by biofouling cover which was influenced by seasonality, biological lifecycles and organism availability. The 18-month data represents biofouling and corrosion expected in mature fouling communities in the early summer months and therefore represents a situation

that is common on marine structures that have lifetimes of >1 year (e.g. Offshore wind turbines with lifetimes of 20-25 years (Pakenham et al. 2021) and merchant vessels that, under the rules of SOLAS (United Nations 1974), can have up to 5 years between dry docks).

Individual Ascidiens were found to grow to a range of sizes with the largest organism measured *in situ* at 12 months with 45 mm length. This is longer than the 10-30 mm annual growth reported by Millar (1952),

however, the measurements in the present study were carried out remotely (by photographic analysis) and therefore did not involve touch, which would have stimulated them into contracting (as reported by Millar).

After 18 months immersion, juvenile barnacles attached to the coupons were able to complete their metamorphosis and calcify into adults (Figure S2). This appears contrary to the work done by Pyefinch and Mott (1948) who showed that the presence of copper prevents the metamorphosis of barnacles. The barnacle attachment seen after 18-months NSW immersion could have been due to external influences (such as food availability or seawater physiochemistry) but could also have been enabled by the biofouling build up acting as a block to slow the seepage of copper into the local seawater. Equally, it could have been enabled by a reduced release of copper as corrosion rate decreased with increased immersion time (as suggested in a 28-day experiment by Yang et al. (2018) and in Figure S4). Further work could consider why barnacles attached to the NAB coupons did not remain attached until the final month of the 18-month study as this could inform the anti-fouling coating industry and biofouling management.

Effect of position within the Marina on macrofouling

In Millbay Marina, the differences between biofouling seen on coupons immersed at the inner site and coupons immersed at the outer site were significant. The coupons immersed at the outer site were within 2 - 15 m of the marina mouth and were therefore influenced by the physiochemistry and fouling organism availability in the seawater of Plymouth Sound. However, the coupons immersed at the inner site were closest to the inner wall of the marina and to the storm drain outlet (Figure 1). During periods of high rainfall, the inner site may have experienced reduced salinity and increased pollution.

In the first 12 months, the inner site coupons were predominantly fouled by Ascidians (particularly *Ciona intestinalis*) whilst the outer site coupons had a larger proportion of Bryozoans and a more diverse fouling community including sponges and star ascidians (*Botryllus* spp. Figure 6). The differences in the biofouling communities seen on the coupons in the inner, middle and outer sites illustrate the significant effects of small-scale geographical and temporal differences in larvae availability, anthropogenic disturbance and seawater physiochemistry. However, the role

of biofilms on larval settlement cannot be excluded (Cacabelos et al. 2020).

The inner and middle sites were measured to have the largest percentage cover of black soot after sandblasting of the nearby marina pilings. However, no relationship was found between the surface area covered by black deposit and the surface area covered by macrofouling organisms or corrosion products. Figure 7 shows an increase in the percentage cover of black deposit after 18 months immersion which was mostly due to a large percentage seen on one of the coupons immersed at the outer site (exact position shown in Figure S5). This could be linked to the sedimentation time in the marina, where finer particles take time to coagulate and settle on the coupons. A typical flux profile of particulate carbon in the ocean was shown by Omand et al. (2020) to illustrate this. However, the marina pollution was also observed to be higher on the final day of the 18 months immersion test at the outer site compared to on previous sampling days (Figure S5) and this could have resulted in an increased bacterial load, encouraging oxidation of the coupon at this attachment point. The outer most coupons were not found to be affected by this pollution, possibly due to the flux of seawater from the nearby marina mouth.

In addition, the proximity of coupons to other metals (such as the steel pilings of the Marina wall and the hulls of nearby yachts) could have induced galvanic corrosion. However, the coupons were positioned on the opposite side of the floating dock to the moored yachts (approximately 3 m from the nearest yacht) and the steel pilings were a minimum of 5 m away from the coupons (and these were painted, except during the sandblasting operation). As such, galvanic corrosion would not have been expected to be significant. In contrast, no galvanic corrosion would have occurred on the coupons immersed in the simulated environment as they were immersed within a plastic tank, isolated from metallic equipment that was placed within a separate (sump) tank.

Corrosion rate, severity and biofouling

Overall corrosion product cover after 12 months of immersion was 13.9% (SD = 3%) for NSW immersed coupons ($n=6$) and 0% (SD = 0%) for SSW immersed coupons ($n=4$) and air exposed coupons ($n=3$). This shows that immersion in NSW results in significantly increased corrosion compared to SSW immersion and air exposure.

The differences seen in the surface cover on the weld material compared to the coupons overall (Figure 7) suggest that the weld material is more vulnerable to corrosion and that fouling build up is slower on the weld material. When immersed for between 6 - 16 months, the weld had on average 18 - 88% fewer macrofouling species per unit area than the overall average. This observation was consistent across samples. However, after an immersion time of 18 months, an anomalously high percentage surface area of the weld of one of the coupons in the outer site became fouled, leading to a change in this pattern. This can be seen in the photograph of the outer coupon in Figure 5. This suggests that corrosion protection methods should be focussed on weld material whilst antifouling should be focussed on both weld and base material.

Evaluation of the corrosion and biofouling maps alongside photographic observations evidences corrosion pits underneath corrosion product deposits and macrofouling organisms (50% of the corroded areas shown in Figure S6 were also biofouled).

The results show increasing weight loss with immersion time when immersion times ≥ 6 months and an initially accelerated corrosion when immersion time = 2 months, Figure 9. This variation in corrosion rate for NAB (Figure S4) supports Oakley et al. (2007) who showed that, after 12 months immersion in natural seawater, corrosion rates stabilised due to corrosion product and marine sediment build-up. Similarly, Wharton and Stokes (2008) suggested that the faster initial corrosion rates were due to corrosion occurring before the development of a mature protective oxide film.

The local hydrodynamics in the marina (due to currents, wave and tidal action) will effect the rate of sedimentation and also alter the corrosion rates (Ault 1995; Wood 2007). As there is only a low flow rate within Millbay Marina (due to the protective marina wall), there will have been increased sedimentation and reduced hydrodynamically initiated erosion-corrosion compared to an open-sea environment. As such, the results could underestimate corrosion rates of NAB in service in an open-sea environment where it is exposed to a higher seawater flow rate. For example, previous research has investigated the effect of erosion-corrosion on friction stir-processed chromium-reinforced NAB composites (Dutta et al. 2022) and the effect of cavitation induced erosion (Li et al. 2021).

The high corrosion rate calculated for the coupon immersed in NSW for 2 months represents a worst-case scenario due to the immersion being carried out in the spring and early summer when some bacterial clades

(such as bacteria in the Order *Rhodobacterales*, which is known to be present in Plymouth, U.K. (Gilbert et al. 2012)) will have been at their peak (Mestre et al. 2020). The results confirm the presence of a biofilm and SRB and there are numerous reports describing increased corrosion in the presence of bacterial metabolites (Scotto et al. 1985) and enzymes (such as catalase) within the EPS of the biofilm (Schiffrin and De Sanchez 1985). SRB have been particularly implicated in examples of accelerated corrosion (Beech 2003; Videla et al. 2005; Videla and Herrera 2005).

The overall corrosion rates calculated assume that a weld bead is present and that no material protection is in place and therefore represent a worse-case scenario. This is important as corrosion protection such as paint can be chipped off as seen in the sinking of the vessel *Ms Nancy C* where pitting and wastage around a forward access cover contributed to the sinking of the vessel (National Transportation Safety Board 2019).

Corrosion rates calculated from the SSW study were a factor of 10 times lower than the corrosion rates calculated from the NSW study. This is because they do not include the corrosion caused by the additional factors found in the natural seawater (including microbially induced corrosion (MIC), crevice corrosion caused by macrofouling organisms, tribocorrosion, temperature, salinity and oxygen concentration variations with time and season etc.). Therefore, corrosion rates calculated from SSW tank tests should be used with caution when predicting the behaviour of metallic components immersed in NSW.

Sea wetted cast NAB components used in U.K. Naval Defence applications must be validated following the requirements of Defence Standard 02-872 Part 2 before service. The purpose of validation is to establish the integrity of the component and create baseline measurements for wall thickness and weld repairs. Defence Standard 02-879 Part 1 Issue 1 states the corrosion rate of NAB to be $0.05-0.075 \text{ mm.yr}^{-1}$. Based on the results shown in the present study, basing validation requirements on this corrosion rate may lead to the underprediction of wall thickness loss per year.

Once cast NAB components have been used in service involving contact with seawater, revalidation of the component (to allow component re-installation following a long overhaul (dry-dock) period) is carried out following Defence Standard 02-872 Part 3. This revalidation establishes the extent of corrosion, the status of any weld repairs and determines the remaining wall thickness. If revalidation of a component is accepted, it will be re-installed on the vessel for continued service.

Revalidation is accepted when all critical wall thicknesses are >90% of the finished machined drawing. When this criterion is not met, revalidation can also be accepted using the probabilistic approach and the MoD developed a code (NABWETIFE) based on a submarine specific database of castings and inspection timescales for this purpose. When NABWETIFE cannot be applied, a deterministic approach (using FEA and fracture mechanics) can be implemented to suggest revalidation acceptance. In this instance, where SSW based corrosion rates are being used as part of the deterministic approach, and based on the results presented here, it is recommended that a 10x corrosion rate factor is included to take account of the effects of biofouling.

Method and testing environments

Wells et al. (2015) summarised time-lapsed corrosion and biofouling data using a thematic coding method. They had small samples where only one code was allocated to each sample and the sampling occurred daily for 43 days. In this study, their method was developed to allow quantification of the photographic output by mapping percentage surface area cover of each theme.

The mapping of the biofouling organisms involved inherent and unavoidable inaccuracies due to the movement and different colour morphology of the organisms. Hydroids and erect Bryozoans stand perpendicular to the coupon surface when immersed in seawater but can relax down onto the coupon surface in air and the colour and texture of Hydroids and sediment are similar. Due to this Hydroid presence was marked as a binary “present or not present” in the early months and then considered as part of the “sediment and Hydroid” percentage coverage once present. Surface area mapping of Ascidians also involved inherent inaccuracies as the surface area covered by each individual organism varied depending on the contraction of the organism’s muscles, how full the organism’s gut was and whether it had flopped over onto its side when it was removed from the water or fallen in on itself longitudinally. However, the comparability of all image based measurements was ensured through consistency in personnel, method and software across all measurements.

The surface cover method used in this paper shows a 2D output for a 3D process. As such, vertical build-up of corrosion products and biofouling is not considered, and this data does not capture where erect Bryozoans flopped on top of nearby Ascidians or where hydroid growth obscured corrosion products.

To avoid this, underwater scans could have been used; however the inherent inaccuracies in capturing moving organisms on a coupon hanging in the water column would also have produced errors.

The testing environment for any corrosion or biofouling study is key and, can typically be identified as “natural seawater” (NSW) or “simulated seawater” (SSW) (The Aluminium Bronze Advisory Service 1981). SSW used in corrosion experiments is well characterised by ASTM D1141-98 (ASTM International 1998) whilst test carried out in NSW (e.g. (Videla et al. 2005)) are exposed to natural fluctuations in parameters including seawater temperature, salinity, nitrate and sulphate concentrations, oxygen concentrations, light etc.

Due to the cost and access issues created by carrying out natural seawater immersion studies in the marine environment, SSW tank studies are often used preferentially. For example, Ault (1995) carried out a corrosion study in an SSW tank as it allowed them to alter the flow rate over the samples whilst controlling other corrosion factors such as water temperature, salinity and pH. Similarly, Wojcik et al. (1997) used an SSW tank with an impinging jet system and continuous, in-situ corrosion potential monitoring which would have been prohibitively difficult to set up in the real marine environment. However, we observed a significant difference in the overall corrosion rate between coupons immersed in NSW, SSW and air. This stands as an example of the importance of representative testing environments, supporting the findings of Mele et al. (1989) and Oakley et al. (2007).

Conclusions

Marine biofouling profoundly affects corrosion rates of welded NAB. Plasma-welded NAB immersed in natural seawater experienced macrofouling which was widespread and well-developed, in addition to a biofilm with density of $20.8 \mu\text{g mm}^{-2}$ and confirmed presence of sulphate-reducing bacteria. Furthermore, juvenile barnacles (*Balanus crenatus*) were able to metamorphose into calcified adults when attached to NAB material that had been immersed in natural seawater for 18 months. The effect of these macrofouling and microfouling organisms (along with the difference in physiochemistry between natural and simulated seawater) increased the corrosion of NAB relative to NAB exposed to the simulated environment. The corrosion rate of NAB immersed in natural seawater was accelerated in the initial 2 months and the average rate over 18 months was calculated as 10

times faster than NAB immersed in simulated seawater and 30 times faster than NAB exposed to air.

Since biofouling can accelerate corrosion in NAB so severely, corrosion rates calculated from simulated seawater tank tests should only be used with extreme caution when predicting life expectancy of metals immersed in natural seawater. As the purpose of corrosion testing is to allow behaviour predictions for metals used in the natural marine environment, it is important to carry out tests in natural seawater where possible and use the results of these tests for life expectancy predictions. This will ensure that all natural variables (such as wind, seawater hydrodynamics, temperature, biofouling and salinity) are included in the predictions.

Acknowledgements

PML Applications Ltd. supported this work through the provision of laboratory space and equipment and by collecting the environmental monitoring data from Millbay Marina. The plasma welding process was developed and performed by Cranfield University and special thanks go to Kuladeep Rajamudili and Supriyo Ganguly for their work on this.

Disclosure statement

No potential conflict of interest was reported by the author(s).

CRedit authorship contribution statement

Tamsin Dobson: Conceptualization, Investigation, Formal analysis, Visualization, Writing - original draft, Writing - review & editing, Project administration, Funding acquisition.

Anna Yunnice: Validation, Writing - review & editing.

Dimitrios Kaloudis: Methodology, Writing - review and editing.

Nicolas Larrosa: Writing - review and editing.

Harry Coules: Writing - review and editing, Supervision, Funding acquisition.

Funding

This work was supported by the EPSRC under Grant [EP/R513179/1] and Babcock International under Studentship [2019 - 4720].

References

Ahmad Z. 2006. Selection of materials for corrosion environment. In: Ahmad ZBT-P of CE and CC, editor. *Princ Corros Eng Corros Control* [Internet]. Oxford: Butterworth-Heinemann; p. 479-549. doi: [10.1016/B978-075065924-6/50010-6](https://doi.org/10.1016/B978-075065924-6/50010-6).

Aljohani TA, Alateyah AI, El-Sanabary S, El-Garaihy WH. 2023. Chapter 16 - Corrosion of weldments [Internet]. In: Khoshnaw FBT-W of MM, editor. Elsevier; p. 565-588. doi: [10.1016/B978-0-323-90552-7.00010-9](https://doi.org/10.1016/B978-0-323-90552-7.00010-9).

ASTM International. 1998. D1141-98 (2021) standard practice for the preparation of substitute ocean water. West Conshohocken (PA): ASTM International. doi: [10.1520/D1141-98R08.2](https://doi.org/10.1520/D1141-98R08.2).

ASTM. 1985. Standard practice for preparing, cleaning, and evaluating corrosion test specimens. ASTM G1-03 (Reapproved 2017). 505-510. doi: [10.1520/G0001-03R17E01.2](https://doi.org/10.1520/G0001-03R17E01.2).

ASTM. 2012. Standard guide for laboratory immersion corrosion testing of metals. ASTM Int. G31-12a:1-10. doi: [10.1520/G0031-21.2](https://doi.org/10.1520/G0031-21.2).

Ault JP. 1995. Erosion corrosion of nickel aluminum bronze in flowing seawater. In *Corros '95 NACE Int Annu Conf Corros Show*. Houston: NACE; p. Paper281.

Beech IB. 2003. Biocorrosion: role of sulfate reducing bacteria. In: Bitton G, editor. *Encycl Environ Microbiol*. John Wiley & Sons, Ltd; p. 465-475. doi: [10.1002/0471263397](https://doi.org/10.1002/0471263397).

Beech IB, Sunner J. 2004. Biocorrosion: towards understanding interactions between biofilms and metals. *Curr Opin Biotechnol*. 15:181-186. doi: [10.1016/j.copbio.2004.05.001](https://doi.org/10.1016/j.copbio.2004.05.001).

Booth GH. 1964. Sulphur bacteria in relation to corrosion. *J Appl Bacteriol*. 27:174-181. doi: [10.1111/j.1365-2672.1964.tb04825.x](https://doi.org/10.1111/j.1365-2672.1964.tb04825.x).

Cacabelos E, Ramalhosa P, Canning-Clode J, Troncoso JS, Olabarria C, Delgado C, Dobretsov S, Gestoso I. 2020. The role of biofilms developed under different anthropogenic pressure on recruitment of macro-invertebrates. *Int J Mol Sci*. 21:2030. doi: [10.3390/ijms21062030](https://doi.org/10.3390/ijms21062030).

Cerchier P, Pezzato L, Gennari C, Moschin E, Moro I, Dabalà M. 2020. PEO coating containing copper: a promising anticorrosive and antifouling coating for seawater application of AA 7075. *Surf Coatings Technol*. 393:125774. doi: [10.1016/j.surfcoat.2020.125774](https://doi.org/10.1016/j.surfcoat.2020.125774).

Chahouri A, Elouahmani N, Ouchene H. 2022. Recent progress in marine noise pollution: a thorough review. *Chemosphere* [Internet]. 291:132983. doi: [10.1016/j.chemosphere.2021.132983](https://doi.org/10.1016/j.chemosphere.2021.132983).

Characklis WG. 1989. Biofilms and corrosion: a process analysis viewpoint. *Int Biodeteriation*. 25:323-326. doi: [10.1016/0265-3036\(89\)90012-2](https://doi.org/10.1016/0265-3036(89)90012-2).

Cobo I, Biezma-Moraleda MV, Linhardt P. 2022. Corrosion evaluation of welded nickel aluminum bronze and manganese aluminum bronze in synthetic sea water. *Mater Corrosion*. 73:1788-1799. doi: [10.1002/maco.202213328](https://doi.org/10.1002/maco.202213328).

Culpan EA, Foley AG. 1982. The detection of selective phase corrosion in cast nickel aluminium bronze by acoustic emission techniques. *J Mater Sci*. 17:953-964. doi: [10.1007/BF00543513](https://doi.org/10.1007/BF00543513).

Delauney L, Compère C, Lehaitre M. 2010. Biofouling protection for marine environmental sensors. *Ocean Sci*. 6:503-511. doi: [10.5194/os-6-503-2010](https://doi.org/10.5194/os-6-503-2010).

Dexter SC. 1988. The use of synthetic environments for corrosion testing. In: Francis PE, Lee TS, editors. *ASTM STP 970*. Philadelphia: American Society for Testing and Materials; p. 217.

- Dexter SC. 1993. Role of microfouling organisms in marine corrosion. *Biofouling*. 7:97–127. doi: [10.1080/08927019309386247](https://doi.org/10.1080/08927019309386247).
- Dobson T, Larrosa N, Kabra S, Coules H. 2022. The role of surface roughness on pitting corrosion initiation in nickel aluminium bronzes in air. *Proc Int Conf Offshore Mech Arct Eng - OMAE*. 3:1–12. doi: [10.1115/OMAE2022-80997](https://doi.org/10.1115/OMAE2022-80997).
- Durante KM. 1991. Larval behavior, settlement preference, and induction of metamorphosis in the temperate solitary ascidian *Molgula citrina* Alder & Hancock. *J Exp Mar Bio Ecol*. 145:175–187. doi: [10.1016/0022-0981\(91\)90174-U](https://doi.org/10.1016/0022-0981(91)90174-U).
- Dutta V, Thakur L, Singh B, Vasudev H. 2022. A study of erosion corrosion behaviour of friction stir-processed chromium-reinforced NiAl bronze composite. *Materials (Basel)*. 15:5401. doi: [10.3390/ma15155401](https://doi.org/10.3390/ma15155401).
- ECHA. 2016. Sig Sulphide Test Data Sheet [Internet].: EP017 110717. https://echamicrobiology.com/app/uploads/2016/06/EP90_Sig-Sulphide-Product-Data-Sheet_180717.pdf.
- Feely RA, Orr J, Fabry VJ, Kleypas JA, Sabine CL, Langdon C. 2009. Present and future changes in seawater chemistry due to ocean acidification. In: Carbon sequestration its role glob carbon cycle [Internet]. Washington (DC): American Geophysical Union. pp. 175–188. doi: [10.1029/2005GM000337](https://doi.org/10.1029/2005GM000337).
- First MR, Policastro SA, Strom MJ, Riley SC, Robbins-Wamsley SH, Drake LA. 2014. 3D imaging provides a high-resolution, volumetric approach for analyzing biofouling. *Biofouling [Internet]*. 30:685–693. doi: [10.1080/08927014.2014.904293](https://doi.org/10.1080/08927014.2014.904293).
- Flemming H-C. 2011. Microbial biofouling: unsolved problems, insufficient approaches, and possible solutions. In: Flemming H-C, Wingender J, Szewzyk U, editors. *Biofilm highlights Springer ser biofilms*, vol 5 [Internet]. Berlin, Heidelberg: Springer Berlin Heidelberg; p. 81–109. doi: [10.1007/978-3-642-19940-0_5](https://doi.org/10.1007/978-3-642-19940-0_5).
- Frankel GS. 1998. Pitting corrosion of metals: a review of the critical factors. *J Electrochem Soc*. 145:2186–2198. doi: [10.1149/1.1838615](https://doi.org/10.1149/1.1838615).
- Gilbert JA, Steele JA, Caporaso JG, Steinbrück L, Reeder J, Temperton B, Huse S, McHardy AC, Knight R, Joint I, et al. 2012. Defining seasonal marine microbial community dynamics. *ISME J*. 6:298–308. doi: [10.1038/ismej.2011.107](https://doi.org/10.1038/ismej.2011.107).
- Hackl R, Hansson J, Norén F, Stenberg O, Olshammar M. 2018. Cultivating *Ciona intestinalis* to counteract marine eutrophication: Environmental assessment of a marine biomass based bioenergy and biofertilizer production system. *Renew Energy*. 124:103–113. doi: [10.1016/j.renene.2017.07.053](https://doi.org/10.1016/j.renene.2017.07.053).
- Hughes RG. 1983. The life-history of *Tubularia indivisa* (Hydrozoa: tubulariidae) with observations on the status of *T. ceratogyne*. *J Mar Biol Ass*. 63:467–479. doi: [10.1017/S0025315400070806](https://doi.org/10.1017/S0025315400070806).
- Krogstad HN, Johnsen R. 2017. Corrosion properties of nickel-aluminium bronze in natural seawater—Effect of galvanic coupling to UNS S31603. *Eval Program Plann [Internet]*. 121:43–56. doi: [10.1016/j.corsci.2017.03.016](https://doi.org/10.1016/j.corsci.2017.03.016).
- Kushkevych I, Hýžová B, Vítězová M, Rittmann SKMR. 2021. Microscopic methods for identification of sulfate-reducing bacteria from various habitats. *Int J Mol Sci*. 22:4007. doi: [10.3390/ijms22084007](https://doi.org/10.3390/ijms22084007).
- Lambert G. 2007. Invasive sea squirts: a growing global problem. *J Exp Mar Bio Ecol*. 342:3–4. doi: [10.1016/j.jembe.2006.10.009](https://doi.org/10.1016/j.jembe.2006.10.009).
- Li Y, Lian Y, Sun Y. 2021. Synergistic effect between cavitation erosion and corrosion for friction stir processed NiAl bronze in artificial seawater. *Met Mater Int*. 27:5082–5094. doi: [10.1007/s12540-020-00916-1](https://doi.org/10.1007/s12540-020-00916-1).
- Little BJ, Lee JS. 2007. *Microbially induced corrosion*. New Jersey: John Wiley & Sons, Inc. doi: [10.1002/047011245X](https://doi.org/10.1002/047011245X).
- Little BJ, Lee JS, Ray RI. 2008. The influence of marine biofilms on corrosion: a concise review. *Electrochim Acta*. 54:2–7. doi: [10.1016/j.electacta.2008.02.071](https://doi.org/10.1016/j.electacta.2008.02.071).
- Little B, Wagner P, Jacobus J. 1988. Impact of sulfate-reducing bacteria on welded copper-nickel seawater piping systems. *Mater Perform*. 27:57–61.
- Little B, Wagner P, Jacobus J, Janus L. 1989. Evaluation of microbiologically induced corrosion in an estuary. *Estuaries [Internet]*. 12:138–141. doi: [10.2307/1351817](https://doi.org/10.2307/1351817).
- Lombardi C, Taylor PD, Cocito S. 2020. Bryozoans: the ‘Forgotten’ bioconstructors. In: Rossi S, Bramanti L, editors. *Perspect Mar Anim For World [Internet]*. Cham: Springer International Publishing; p. 193–217. doi: [10.1007/978-3-030-57054-5_7](https://doi.org/10.1007/978-3-030-57054-5_7).
- Maul GA, Davis AM, Simmons JW. 2001. Seawater temperature trends at Usa Tide Gauge sites. *Geophys Res Lett [Internet]*. 28:3935–3937. doi: [10.1029/2001GL013458](https://doi.org/10.1029/2001GL013458).
- Mele MFLD, Brankevich G, Videla HA. 1989. Corrosion of CuNi30Fe in artificial solutions and natural sea water: influence of biofouling. *Br Corros J*. 24:211–218. doi: [10.1179/000705989798269993](https://doi.org/10.1179/000705989798269993).
- Meng Y, Li C, Li H, Shih K, He C, Yao H, Thiyagarajan V. 2019. Recoverable impacts of ocean acidification on the tubeworm, *Hydroides elegans*: implication for biofouling in future coastal oceans. *Biofouling*. 35:945–957. doi: [10.1080/08927014.2019.1673376](https://doi.org/10.1080/08927014.2019.1673376).
- Mestre M, Höfer J, Sala MM, Gasol JM. 2020. Seasonal variation of bacterial diversity along the marine particulate matter continuum. *Front Microbiol*. 11:1590. doi: [10.3389/fmicb.2020.01590](https://doi.org/10.3389/fmicb.2020.01590).
- Millar RH. 1952. The annual growth and reproductive cycle in four ascidians. *J Mar Biol Ass*. 31:41–61. [accessed 2023 May 14]. doi: [10.1017/S0025315400003672](https://doi.org/10.1017/S0025315400003672).
- Ministry of Defence. 2013. Defence Standard 02-747 Part 2 requirements for Nickel Aluminium Bronze castings and ingots Part 2: Nickel Aluminium Bronze Naval alloy ingots and sand casting with welding permitted to the wetted surface. Glasgow: UK Defence Standardization.
- Ministry of Defence. 2018. Defence Standard 02-833 Part 02 requirements for Nickel Aluminium Bronze Part : 02 : forgings, forging stock, rods & sections. Glasgow: UK Defence Standardization.
- National Transportation Safety Board. 2019. Safety brief: flooding and sinking of towing vessel Ms Nancy C. USA: National Transportation Safety Board. doi: [10.5749/j.ctvthhd37.29](https://doi.org/10.5749/j.ctvthhd37.29).
- Neodo S, Carugo D, Wharton JA, Stokes KR. 2013. Electrochemical behaviour of nickel–aluminium bronze in chloride media: influence of pH and benzotriazole. *J Electroanal Chem [Internet]*. 695:38–46. [accessed 2019 Oct 3]. doi: [10.1016/j.jelechem.2013.02.007](https://doi.org/10.1016/j.jelechem.2013.02.007).

- Noori R, Tian F, Berndtsson R, Abbasi MR, Naseh MV, Modabberi A, Soltani A, Kløve B. 2019. Recent and future trends in sea surface temperature across the Persian Gulf and Gulf of Oman. *PLoS One* [Internet]. 14:e0212790. doi: [10.1371/journal.pone.0212790](https://doi.org/10.1371/journal.pone.0212790).
- Oakley RS, Galsworthy JC, Fox GS, Stokes KR. 2007. Long-term and accelerated corrosion testing methods for cast nickel-aluminium bronzes in seawater. In Féron D, editor. *Corrosion behaviour and protection of copper and aluminium alloys in seawater*. UK: Woodhead Publishing; p. 119–127. doi: [10.1533/9781845693084.3.119](https://doi.org/10.1533/9781845693084.3.119).
- Omand MM, Govindarajan R, He J, Mahadevan A. 2020. Sinking flux of particulate organic matter in the oceans: sensitivity to particle characteristics. *Sci Rep*. 10:5582. doi: [10.1038/s41598-020-60424-5](https://doi.org/10.1038/s41598-020-60424-5).
- Pakenham B, Ermakova A, Mehmanparast A. 2021. A review of life extension strategies for offshore wind farms using techno-economic assessments. *Energies*. 14:1936. doi: [10.3390/en14071936](https://doi.org/10.3390/en14071936).
- Procópio L. 2019. The role of biofilms in the corrosion of steel in marine environments. *World J Microbiol Biotechnol*. 35:73. doi: [10.1007/s11274-019-2647-4](https://doi.org/10.1007/s11274-019-2647-4).
- Pyefinch KA, Mott JC. 1948. The sensitivity of barnacles and their larvae to Copper and Mercury. *J Exp Biol*. 25: 276–298. doi: [10.1242/jeb.25.3.276](https://doi.org/10.1242/jeb.25.3.276).
- Qian PY, Cheng A, Wang R, Zhang R. 2022. Marine biofilms: diversity, interactions and biofouling. *Nat Rev Microbiol*. 20:671–684. doi: [10.1038/s41579-022-00744-7](https://doi.org/10.1038/s41579-022-00744-7).
- Railkin AI. 2004. *Marine biofouling: colonization processes and defenses*. 1st ed. Boca Raton (FL): CRC Press LLC.
- Richardson I. 2016. Guide to Nickel Aluminium Bronze for Engineers [Internet].: 100. https://www.nickelinstitute.org/~media/Files/MediaCenter/News/20160205-Guide_to_Nickel_Aluminium_Bronze_for_Engineers.ashx?la=en.
- Rius M, Branch GM, Griffiths CL, Turon X. 2010. Larval settlement behaviour in six gregarious ascidians in relation to adult distribution. *Mar Ecol Prog Ser*. 418:151–163. doi: [10.3354/meps08810](https://doi.org/10.3354/meps08810).
- Schiffirin DJ, De Sanchez SR. 1985. The effect of pollutants and bacterial microfouling on the corrosion of copper base alloys in seawater. *Corrosion* [Internet]. 41:31–38. doi: [10.5006/1.3581966](https://doi.org/10.5006/1.3581966).
- Schultz MP. 2007. Effects of coating roughness and biofouling on ship resistance and powering. *Biofouling*. 23:331–341. doi: [10.1080/08927010701461974](https://doi.org/10.1080/08927010701461974).
- Schüssler A, Exner HE. 1993. The corrosion of nickel-aluminium bronzes in seawater—I. Protective layer formation and the passivation mechanism. *Corros Sci*. 34: 1793–1802. doi: [10.1016/0010-938X\(93\)90017-B](https://doi.org/10.1016/0010-938X(93)90017-B).
- Scotto V, Cintio RD, Marcenaro G. 1985. The influence of marine aerobic microbial film on stainless steel corrosion behaviour. *Corros Sci* [Internet]. 25:185–194. doi: [10.1016/0010-938X\(85\)90094-0](https://doi.org/10.1016/0010-938X(85)90094-0).
- The Aluminium Bronze Advisory Service. 1981. *Aluminium Bronze Alloys corrosion resistance guide*: publication No: 80. London (UK): Copper Development Association.
- United Nations. 1974. *International convention for the safety of life at sea*. London (UK): International Maritime Organization.
- Videla HA, Herrera LK. 2005. Microbiologically influenced corrosion: looking to the future. *Int Microbiol*. 8:169–180. doi: [10.2436/im.v8i3.9523](https://doi.org/10.2436/im.v8i3.9523).
- Videla HA, Herrera LK, Edyvean RG. 2005. An updated overview of SRB induced corrosion and protection of carbon steel. In: *Corros 2005*. Houston: NACE International; p. 1–11.
- Vinagre PA, Simas T, Cruz E, Pinori E, Svenson J. 2020. Marine biofouling: a European database for the marine renewable energy sector. *JMSE*. 8:495. doi: [10.3390/jmse8070495](https://doi.org/10.3390/jmse8070495).
- Vuong P, McKinley A, Kaur P. 2023. Understanding biofouling and contaminant accretion on submerged marine structures. *Npj Mater Degrad*. 7:50. doi: [10.1038/s41529-023-00370-5](https://doi.org/10.1038/s41529-023-00370-5).
- Webster BJ, Newman RC. 1994. Microbiologically Influenced Corrosion Testing. In: Kearns JR, Little BJ, editors. *ASTM STP 1232*. Philadelphia: American Society for Testing and Materials; p. 28.
- Wells N, Martinez C, Bass M, Moon R. 2015. Metal corrosion: A qualitative analysis. *Forensic Engineering* 2015. *Proceedings of the 7th Congress of Forensic Engineering*; December; 693–704. doi: [10.1061/9780784479711.068](https://doi.org/10.1061/9780784479711.068).
- Wharton JA, Barik RC, Kear G, Wood RJK, Stokes KR, Walsh FC. 2005. The corrosion of nickel-aluminium bronze in seawater. *Corros Sci*. 47:3336–3367. doi: [10.1016/j.corsci.2005.05.053](https://doi.org/10.1016/j.corsci.2005.05.053).
- Wharton JA, Stokes KR. 2008. The influence of nickel-aluminium bronze microstructure and crevice solution on the initiation of crevice corrosion. *Electrochim Acta*. 53: 2463–2473. doi: [10.1016/j.electacta.2007.10.047](https://doi.org/10.1016/j.electacta.2007.10.047).
- Wojcik PT, Charriere E, Orazem ME. 1997. Experimental study of the erosion-corrosion of Copper and Copper-Nickel Alloys at the corrosion potential and at anodic potentials. In: Tri Service Committee on Corrosion, editor. 1997 Tri-Service Conf Corros [Internet]. Wrightsville Beach, NC: The Department of Defense; p. 1–15. <https://apps.dtic.mil/sti/pdfs/ADA332666.pdf>.
- Wolfgong WJ. 2016. Chapter 14 - Chemical analysis techniques for failure analysis: part 1, common instrumental methods. In: *Handb Mater Fail Anal with Case Stud from Aersp Automot Ind*. Butterworth-Heinemann; p. 279–307. doi: [10.1016/B978-0-12-800950-5.00014-4](https://doi.org/10.1016/B978-0-12-800950-5.00014-4).
- Wood RJK. 2007. Erosion–corrosion interactions of copper and aluminium alloys. In: Féron D, editor. *Corrosion behaviour and protection of copper and aluminium alloys in seawater*. UK: Woodhead Publishing; p. 19–44. doi: [10.1533/9781845693084.1.19](https://doi.org/10.1533/9781845693084.1.19).
- Wood RJK. 2017. Marine wear and tribocorrosion. *Wear* [Internet]. 376–377:893–910. doi: [10.1016/j.wear.2017.01.076](https://doi.org/10.1016/j.wear.2017.01.076).
- Xometry. 2018. Selecting right surface roughness for CNC machining [Internet]. [accessed 2023 Sep 25]. <https://xometry.eu/en/selecting-right-surface-roughness-for-cnc-machining/>.
- Yang F, Kang H, Guo E, Li R, Chen Z, Zeng Y, Wang T. 2018. The role of nickel in mechanical performance and corrosion behaviour of nickel-aluminium bronze in 3.5 wt.% NaCl solution. *Corros Sci* [Internet]. 139:333–345. [accessed 2019 Nov 14]. <https://www.sciencedirect.com/science/article/pii/S0010938X18300490>. doi: [10.1016/j.corsci.2018.05.012](https://doi.org/10.1016/j.corsci.2018.05.012).
- Yruela I. 2005. Copper in plants. *Braz J Plant Physiol*. 17: 145–156. doi: [10.1590/S1677-04202005000100012](https://doi.org/10.1590/S1677-04202005000100012).
- Zobell CE, Allen EC. 1935. The significance of marine bacteria in the fouling of submerged surfaces. *J Bacteriol*. 29: 239–251. doi: [10.1128/jb.29.3.239-251.1935](https://doi.org/10.1128/jb.29.3.239-251.1935).